DESY 94-197
hep-ph/9411217

Towards the Phenomenology of QCD–Instanton Induced Particle Production at HERA*

A. Ringwald and F. Schrempp

Deutsches Elektronen-Synchrotron DESY, Hamburg, Germany

Abstract

We present a first status report on a broad and systematic study of possible manifestations of QCD-instantons at HERA. Considerable motivation comes from the close analogy between instanton-induced $B+L$ violation in electroweak processes and effects of QCD-instantons in deep inelastic scattering. We concentrate on the high multiplicity final state structure, reminiscent of an isotropically decaying "fireball". A set of experimental isolation criteria is proposed. They serve to further enhance the striking event signature without significantly suppressing the expected rates.

*to pe published in Proc. of the International Seminar "Quarks–94", Vladimir/Russia, May 11-18, 1994

1 Introduction

The basic significance and possible importance of QCD-instanton effects in deep inelastic scattering for decreasing Bjorken variable $x_{\rm Bj}$ and high photon virtuality Q^2 has recently been emphasized [1].

First of all, it has been argued [2, 1] that the calculable small scale instanton dynamics [3] may be factorized from the large distance effects, allowing for a semiquantitative estimate of instanton-induced contributions to the structure functions [1] and the hadronic final state [4]. This is rooted in the fact that $1/\sqrt{Q^2}$ plays the rôle of a dynamical infrared cut-off for the instanton size [3].

Secondly, QCD-instanton effects for decreasing $x_{\rm Bj}$ are largely analogous to the manifestation of electroweak instantons for increasing energies [3]. The anomalous $B+L$ violation due to electroweak instantons is paralleled by a chirality violation induced by QCD-instantons [5]. The spectacular possibility of a strong increase of multi-$W^{\pm}/Z^0$ production in the multi-TeV regime [6, 7] due to electroweak instantons corresponds to a strong enhancement of multi-gluon production at small $x_{\rm Bj}$ due to QCD-instantons. Striking consequences include a high multiplicity final state structure, reminiscent of a decaying "fireball".

Whereas a promising search for anomalous electroweak events is only possible in the far future, presumably at a post-LHC collider [8] or at cosmic ray facilities [9], the search for anomalous events induced by QCD-instantons can start right now, in deep inelastic $e^{\pm}p$ scattering at HERA.

The present paper represents a first status report on a broad and systematic study of possible manifestations of QCD-instantons which could be searched for at HERA [4]. While a theoretical derivation of crucial quantities characterizing the instanton-induced final state ($1, 2 \ldots$ particle inclusive rates, average multiplicity, average transverse momenta, energy flow, etc.) will be deferred to Ref. [4], we mainly report here on the phenomenological aspects of our results.

The organization of this contribution is as follows. We start off in Section 2 by expanding on the close analogy between instanton-induced $B+L$ violation in electroweak processes and effects of QCD-instantons in deep inelastic scattering. Section 3 contains a summary of the results of Balitsky and Braun [1] concerning the QCD-instanton induced contribution to the gluon and quark structure functions. We also emphasize the approximations and limitations inherent in this calculation. Furthermore, we present the instanton contribution to the nucleon structure function $F_2(x_{\rm Bj}, Q^2)$ ob-

tained by convoluting the results of Ref. [1] with phenomenological distributions of quarks and gluons in the nucleon. In Section 4 we report on our ongoing investigation [4] of the QCD-instanton induced hadronic final state in deep inelastic scattering. The main emphasis rests on the characteristic event topology along with a discussion of experimental isolation criteria, serving to further enhance the striking event signature without significantly suppressing the rates. A search strategy for instanton-induced events is formulated. In Section 5, we present a summary and an outlook on related aspects and open problems under study.

2 The QFD – QCD Connection

The Standard Model of electroweak (QFD) and strong (QCD) interactions is remarkably successful. In particular, its perturbative formulation ("Feynman diagrammatics") appears to be theoretically consistent and agrees with precision experiments (where applicable, i.e. for small coupling constant).

Nevertheless, even for small couplings, there exist physical processes which cannot be described by conventional perturbation theory, notably, phenomena associated with *quantum tunnelling*.

In non-Abelian gauge theories such as QFD and QCD the vacuum actually has a complicated structure, even on the classical level [10]: The potential energy is periodic with respect to the so-called Chern-Simons number (c.f. Fig. 1),

$$N_{\rm CS}[A] = \frac{g^2}{16\pi^2}\int d^3x\ \epsilon_{ijk}\left(A_i^a\partial_j A_k^a - \frac{g}{3}\epsilon_{abc}A_i^a A_j^b A_k^c\right), \qquad (1)$$

which is the (topological) winding number of the (non-Abelian) gauge field (A) under consideration. Pure gauge fields corresponding to the degenerate minima of the potential energy (perturbative vacua) have integer values of the Chern-Simons number $N_{\rm CS}$. Moreover, pure gauge fields differing by $\triangle N_{\rm CS} = n =$ integer are topologically inequivalent. They are related to each other by a topologically non-trivial static gauge transformation with winding number n. This means that they are separated by an energy barrier, as shown schematically in Fig. 1.

In the electroweak theory a mass scale, $v \approx 246$ GeV, is introduced via spontaneous symmetry breaking and, correspondingly, there is a definite

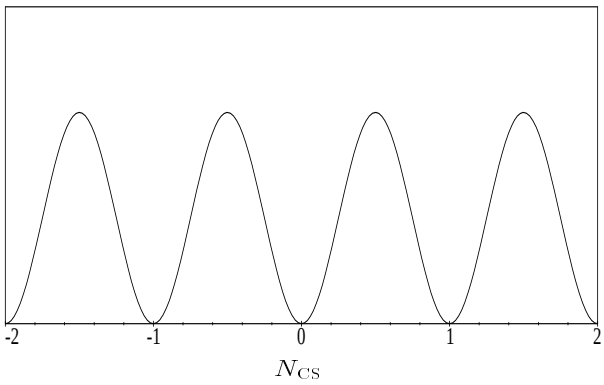

Figure 1: Schematic illustration of the static potential energy of the gauge (and Higgs) field vs. the Chern-Simons number

minimum barrier height associated with the W-mass, of order [11]

$$M_{\rm barrier}^{\rm QFD} \sim \frac{m_W}{\alpha_W} \sim \mathcal{O}(10\ {\rm TeV}). \tag{2}$$

As is well known, this minimum barrier energy is associated with a certain static, unstable solution to the classical field equations, the so-called 'sphaleron' [11]. It may be viewed [12] as an intermediate, coherent field configuration consisting of a large number, $\mathcal{O}(1/\alpha_W)$, of W/Z (and Higgs) bosons, confined to a characteristic volume of order m_W^{-3}.

In QCD, being an "unbroken" gauge theory, the minimum barrier height depends on the considered process and its kinematics. It turns out, that the notion of the minimum barrier may be qualitatively transcribed from QFD, provided that there is a (process dependent) hard scale Q' available. Specifically, in deep inelastic $e^{\pm}p$ scattering,

$$Q'^2 \propto Q^2 = -({\rm mass})^2 \ \ \text{of the virtual photon.} \tag{3}$$

Besides $\alpha_W \to \alpha_s$, one is then led to substitute the characteristic linear dimension [3, 2, 1, 13]

$$\frac{1}{m_W} \to \frac{1}{\alpha_s(Q')Q'}. \tag{4}$$

The minimum barrier energy (from Eqs. $(2,4)$)

$$M_{\rm barrier}^{\rm QCD} \sim Q', \tag{5}$$

is now associated with a sphaleron-like intermediate, coherent field configuration consisting of a large number, $\mathcal{O}(1/\alpha_s)$, of gluons in a characteristic volume $(\alpha_s Q')^{-3}$.

Transitions between minima of the effective potential in Fig. 1 lead to a violation of fermionic quantum numbers in the Standard Model [5, 14]. In particular, baryon (B) and lepton (L) number conservation is violated due to non-perturbative electroweak gauge fields (W) associated with the SU(2) flavour gauge group, according to the selection rule

$$\triangle L_{e,\mu,\tau} = \frac{1}{3}\triangle B = -\triangle N_{\rm CS}[W]. \tag{6}$$

In analogy, non-perturbative gluon fields (G) associated with the SU(3) colour gauge group induce a violation of chirality conservation for (massless) quarks,

$$\triangle Q^5_{u,d,s,\ldots} = 2\ \triangle N_{\rm CS}[G]. \tag{7}$$

For parton-parton center of mass (c.m.) energies[1] $\sqrt{s'} < M_{\rm barrier}$, such processes are classically forbidden and only occur via quantum tunnelling under the barrier in Fig. 1. In this case, the sphaleron-like intermediate state corresponding to the energies (2), (5) can only be reached virtually. Correspondingly, the respective cross sections are exponentially suppressed in the coupling [5],

$$\sigma_{\rm tunnelling} \sim \exp(-4\pi/\alpha)\,; \quad \alpha = \alpha_W, \alpha_s. \tag{8}$$

Let us recall the origin of this tunnelling suppression factor in somewhat more detail. The amplitude of anomalous fermion number violating processes can be obtained by expanding the path integral for the corresponding Green's functions about *instantons* [15, 5, 16], which are classical solutions of the Yang-Mills(-Higgs) equations in 4-dimensional Euclidean space with finite action. The instanton (I) (anti-instanton ($\overline{I}$)) may be viewed as a most probable tunnelling solution, interpolating in Euclidean time between the gauge (and Higgs) field configurations of two neighbouring vacua with $\triangle N_{\rm CS} = +1(-1)$. It passes the above-mentioned sphaleron-like intermediate state in-between.

[1] Henceforth, we shall denote by $\sqrt{s'}$ the total c.m. energy of the non-perturbative subprocess, while $\sqrt{s}$ refers to the total c.m. energy of the physical process under consideration.

In QCD, for example, the instanton is explicitly given by[2]

$$G_\mu^{(I)}(x-x_I;U_I,\rho_I) = -\frac{\mathrm{i}}{g}\frac{U_I[\sigma_\mu(\bar{x}-\bar{x}_I)-(x-x_I)_\mu]\bar{U}_I}{(x-x_I)^2((x-x_I)^2+\rho_I^2)}\rho_I^2, \qquad (9)$$

depending on a set of collective coordinates $\{x_I, \rho_I, U_I\}$, like center, x_I, size, ρ_I, and orientation in group space, U_I. Since the action is independent (QCD) or only slightly depends (QFD) on these collective coordinates, they are to be integrated over. For the simplest exclusive anomalous processes one obtains (for QFD, see Refs. [5, 6], for QCD, see Refs. [3, 2, 1]) in this way to exponential accuracy:

$\triangle(B+L) = -2n_{\mathrm{family}} = -6$:

$$T\,(qq \to 7\overline{q}3\overline{l}\,) \propto \int d\rho_I \;\; ... \;\; \exp\left[-\frac{2\pi}{\alpha_W(\rho_I^{-1})}S_I^{\mathrm{QFD}}(\rho_I)\right], \qquad (10)$$

$\triangle Q^5 = 2n_f = 6$:

$$\left\{\begin{array}{lcl} T\,(g^*g & \to & 3q_L3\overline{q_R}) \\ T\,(\overline{q_L}^*g & \to & 2q_L3\overline{q_R}) \\ T\,(\overline{q_L}^*q_R & \to & 2q_L2\overline{q_R}) \\ & \cdots & \end{array}\right\} \propto \int d\rho_I \;\; ... \;\; \exp\left[-Q'\rho_I - \frac{2\pi}{\alpha_s(\rho_I^{-1})}S_I^{\mathrm{QCD}}\right], \qquad (11)$$

where, in our normalization, the action of the QCD-instanton is given by $S_I^{\mathrm{QCD}} = 1$, whereas the action of the QFD-instanton reads $S_I^{\mathrm{QFD}} = 1 + (1/2)\rho_I^2 m_W^2$. In the various QCD-instanton induced subprocesses of Eq. (11), the star indicates that the corresponding parton carries a virtuality $Q' = \sqrt{-q'^2} > 0$. We observe that, for exclusive anomalous processes, the instanton size is effectively cut off at $\rho_{\mathrm{cut}} \sim v^{-1}$ in the electroweak theory [5, 16] and at $\rho_{\mathrm{cut}} \sim Q'^{-1}$ in QCD [3, 2, 1] (for early discussions, see Ref. [17]).

Most interesting from a theoretical point of view and in the light of present and future collider experiments is the case $\sqrt{s'} > M_{\mathrm{barrier}}$, where a transition over the barrier is classically allowed, i.e. energetically possible. Unfortunately, the crucial *dynamical* question is still unsettled [7] whether the transition from a state with a few initial partons to the *very different* sphaleron-like multi-parton coherent state can proceed without extra suppression. Only then could such anomalous processes acquire an observable

[2] We use here the notations $\sigma_\mu^{\alpha\dot{\alpha}} = (-i\sigma, 1)$, $\bar{\sigma}_{\mu\dot{\alpha}\alpha} = (+i\sigma, 1)$ (σ are the standard Pauli matrices). Furthermore we abbreviate $x = x_\mu\sigma_\mu, \bar{x} = x_\mu\bar{\sigma}_\mu$, etc.

cross section and the final state would consist of a large number, $\mathcal{O}(\alpha_{W(s)}^{-1})$, of W/Z's (gluons) in addition to the few fermions required by the anomaly.

The possibility that this intriguing scenario might be realized in nature was first observed in the context of the electroweak theory in Ref. [6]. It was found [18] that, to exponential accuracy, the total cross section for anomalous $B+L$ violation, in the high energy and weak coupling limit,

$$\frac{\sqrt{s'}}{m_W} \to \infty, \qquad \frac{\alpha_W \sqrt{s'}}{m_W} \ \text{ fixed}, \tag{12}$$

can be written in the following scaling form

$$\sigma_{\rm QFD}^{(I)\,\rm tot} \propto \exp\left[-\frac{4\pi}{\alpha_W(\rho_*^{-1})}\ F^{\rm QFD}\left(\frac{\sqrt{s'}}{M_0}\right)\right], \tag{13}$$

where $M_0 = \sqrt{6}\pi m_W/\alpha_W$ is of the order of the minimum barrier height Eq. (2). The so-called "holy-grail" function F in the exponent is known only in a low energy expansion whose first few terms are given by [19]

$$F^{\rm QFD}(\epsilon) = 1 - \frac{9}{8}\ \epsilon^{4/3} + \frac{9}{16}\ \epsilon^2 + \mathcal{O}(\epsilon^{8/3}[1+\ln\epsilon]), \tag{14}$$

where $\epsilon = \sqrt{s'}/M_0$. The effective instanton size entering the running coupling in (13) scales like m_W^{-1},

$$\rho_* = \frac{1}{m_W}\left[\sqrt{\frac{3}{2}}\epsilon^{2/3} + \cdots\right]. \tag{15}$$

Note, that the first term in the series expression for the holy grail function, Eq. (14), corresponds to the "naive" tunnelling factor, Eq. (8). Apparently, the total cross section is exponentially growing for $(m_W \ll)\ \sqrt{s'} \ll M_0$, but still small within the region of validity of expansion (14). As anticipated above, in this energy region, it is dominated by the associated production of a large number of W and Z bosons,

$$\langle\ n_W\ \rangle = \frac{\pi}{\alpha_W}\ \left[\frac{3}{2}\ \epsilon^{4/3} + \mathcal{O}(\epsilon^2)\right]. \tag{16}$$

Unfortunately, nothing is known about the behaviour of the holy grail function for $\sqrt{s'}$ around or above the barrier energy $M_{\rm barrier}^{\rm QFD}$. The different terms in the perturbative expansion of $F^{\rm QFD}$ become comparable in size, and the perturbative expansion breaks down, just in this most interesting region.

Unitarity and other arguments along with various assumptions have been used to argue [20] that the decrease of the holy grail function may well level off at values of order $F^{\rm QFD} \simeq 1/2$, leading to unobservably small cross sections of electroweak $B+L$ violation. However, this question is not finally settled.

It is very remarkable that the contribution of QCD-instantons to deep inelastic scattering strongly ressembles Eqs. (13)-(16), as first observed for g^*g scattering in Refs. [3, 2] and elaborated for γ^*g scattering in Ref. [1]. In the Bjorken limit (c.f. Fig. 2 for the kinematics),

$$\left.\begin{array}{c} Q'^2 = -q'^2, \\ \text{c.m. energy}^2 \text{ of } I\text{-subprocess, } s' = (q'+p)^2 \end{array}\right\} \to \infty \; ; \; x' = \frac{Q'^2}{2pq'} \;\; \text{fixed}, \tag{17}$$

the total subprocess cross section for instanton-induced chirality violation is found to have the following structure

$$\sigma_{\rm QCD}^{(I)\,\rm tot} \propto \exp\left[-\frac{4\pi}{\alpha_s(\rho_*^{-1})}\, F^{\rm QCD}(x')\right], \tag{18}$$

where [3, 2, 1]

$$\begin{aligned} F^{\rm QCD}(x') &= 1 - \frac{3}{2}\,\left(\frac{1-x'}{1+x'}\right)^2 + \mathcal{O}\left(\left(\frac{1-x'}{1+x'}\right)^4\left[1+\ln\left(\frac{1-x'}{1+x'}\right)\right]\right), \\ \rho_* &= \frac{4\pi}{\alpha_s(Q')Q'}\left[3\left(\frac{1-x'}{1+x'}\right)^2 + \cdots\right]. \end{aligned} \tag{19}$$

The effective instanton size ρ_* in Eqs. (18,19), acting as the characteristic linear dimension, as well as the scaling form of $F^{\rm QCD}(x')$ are in accordance with the substitution rule (4) from QFD to QCD. The average gluon multiplicity is found to be [4],

$$\langle\, n_g \,\rangle = \frac{\pi}{\alpha_s}\;\left[\,6\left(\frac{1-x'}{1+x'}\right)^2 + \mathcal{O}\left(\left(\frac{1-x'}{1+x'}\right)^3\right)\right]. \tag{20}$$

It is exactly this similarity between QFD and QCD instanton-induced scattering processes which makes the study of the latter at HERA so interesting.

3 Instanton-Induced Contributions to Structure Functions

In this Section, let us sketch the essential steps in the pioneering calculation of QCD-instanton contributions to the (nucleon) structure functions in Ref. [1]. Along the way, we shall emphasize the basic ingredients as well as the inherent limitations. Finally, a state of the art evaluation of the I-induced contribution to the F_2 structure function of the proton will be presented.

First of all, it is argued [1] that the celebrated factorization theorem remains valid beyond conventional perturbation theory and allows to express the instanton contribution to the nucleon structure functions $F_{1,2}$ in the familiar form

$$F_i^{(I)}(x_{\rm Bj},Q^2) = a_i(x_{\rm Bj}) \sum_{p=g,q,\bar{q}} \int_{x_{\rm Bj}}^1 \frac{dx}{x}\; p\left(\frac{x_{\rm Bj}}{x},\mu\right)\; \mathcal{F}_i^{(I)p}\left(x,\frac{Q^2}{\mu^2},\alpha_s(\mu^2)\right). \tag{21}$$

In Eq. (21), $a_1 = 1/2$, $a_2(x_{\rm Bj}) = x_{\rm Bj}$, x is the Bjorken variable of the γ^*-parton subprocess , and μ is the factorization scale separating "hard" and "soft" contributions to the cross section. The distributions $p(z,\mu)$ of partons p in the nucleon absorb all information about the dynamics at large distances and, as usual, are to be taken from experiment. By virtue of Eq. (21), the theoretical efforts in Ref. [1] concentrate on calculating the "parton" structure functions $\mathcal{F}_i^{(I)p}\left(x,\frac{Q^2}{\mu^2},\alpha_s(\mu^2)\right)$ in the instanton background. For a detailed discussion on the familiar and important problem of infrared (IR) divergencies (associated with integrations over the instanton size), we have to refer to Ref. [1]. In summary, it is claimed that these divergencies may be consistently absorbed into the parton distributions $p(z,\,\mu)$, and an unambiguous, IR-protected contribution from small instantons may be isolated.

According to the optical theorem the parton structure functions $\mathcal{F}_i^{(I)p}$ are related to the imaginary part of the forward virtual photon-parton matrix element (c.f. Fig. 2)

$$T_{\mu\nu}^{\rm parton} = {\rm i}\int d^4z\, e^{{\rm i}qz}\,\langle\,{\rm parton}(p),\,\lambda\,|T\{j_\mu(z)j_\nu(0)\}|\,{\rm parton}(p),\,\lambda\,\rangle. \tag{22}$$

The calculation of the instanton-induced contribution to the parton structure functions then involves the following steps:

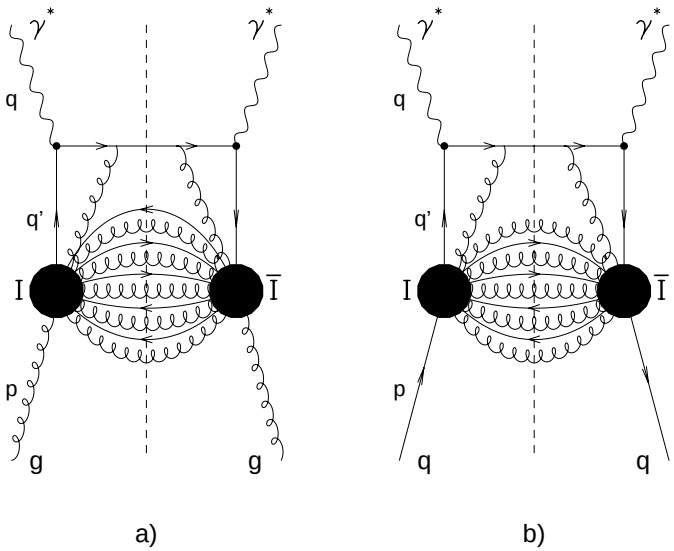

Figure 2: The contribution of an $I\overline{I}$ pair to to the structure function of a gluon (a) and of a quark (b). Solid lines are quark zero modes in the case that they are ending at the instanton (anti-instanton), and quark propagators in the $I\overline{I}$ background otherwise. Note that the black blobs denoted by $I(\overline{I})$ are often referred to in the text as the $I(\overline{I})$-subprocess.

- The path integral expression for the matrix element (22) in Euclidean space is expanded about the instanton/anti-instanton pair configuration, defined via the so-called valley method [3, 21][3].
- Next, the integrations over the large number of collective coordinates associated with the $I\overline{I}$ configuration have to be performed.
- After Fourier transformation, the last step consists in rotating the result to Minkowski space and, thereafter, taking the imaginary part.

After a long and tedious calculation, heavily exploiting the light-cone approximation, Balitsky and Braun [1] succeeded in performing these steps. Their final answer for the instanton-induced contribution to the gluon and

[3]For any fixed values of the collective coordinates $\{\tau\}$, the pair configuration ($I\overline{I}$ "valley") is required to minimize the action within the subspace orthogonal to $\partial G^{I\overline{I}}/\partial\tau_i$.

quark structure functions, derived in the Bjorken limit (c.f. Fig. 2),

$$\left.\begin{array}{c} Q^2 = -q^2, \\ \gamma^*\text{–parton c.m. energy}^2,\ \hat{s} = (q+p)^2 \end{array}\right\} \to \infty\ ;\ x = \frac{Q^2}{2pq}\ \text{ fixed}, \qquad (23)$$

reads:

$$\begin{aligned} \mathcal{F}_{1,2}^{(I)\,g}(x,Q^2) &\simeq \sum_q e_q^2 \frac{1}{9(1-x)^2} \frac{d^2\pi^{9/2}}{bS(\xi_*)[bS(\xi_*)-1]} \left(\frac{16}{\xi_*^3}\right)^{n_f-3} \\ &\quad \times \left(\frac{2\pi}{\alpha_s(\rho_*^{-1})}\right)^{19/2} \exp\left[-\left(\frac{4\pi}{\alpha_s(\rho_*^{-1})} + 2b\right) S(\xi_*)\right], \qquad (24) \end{aligned}$$

$$\begin{aligned} \mathcal{F}_{1,2}^{(I)\,q}(x,Q^2) &\simeq \left[\sum_{q'\neq q} e_{q'}^2 + \frac{1}{2}e_q^2\right] \frac{128}{81(1-x)^3} \frac{d^2\pi^{9/2}}{bS(\xi_*)[bS(\xi_*)-1]} \left(\frac{16}{\xi_*^3}\right)^{n_f-3} \\ &\quad \times \left(\frac{2\pi}{\alpha_s(\rho_*^{-1})}\right)^{15/2} \exp\left[-\left(\frac{4\pi}{\alpha_s(\rho_*^{-1})} + 2b\right) S(\xi_*)\right], \qquad (25) \end{aligned}$$

where e_q are the electric charges of the quarks, $b = 11 - (2/3)n_f$, and $d \simeq 0.00363$ (for $n_f = 3$ massless flavours) is a constant which enters the expression for the instanton density [5].

The classical action of the instanton/anti-instanton pair, $S(\xi)$, is the most important ingredient in Eqs. (24,25), since it enters in the exponent. Due to conformal invariance, it only depends on the following combination [3, 21] of collective coordinates,

$$\xi = \frac{R^2 + \rho_I^2 + \rho_{\overline{I}}^2}{\rho_I \rho_{\overline{I}}}, \qquad (26)$$

with $R^2 = (x_I - x_{\overline{I}})^2$ being the instanton – anti-instanton separation, and $\rho_I, \rho_{\overline{I}}$ their sizes, respectively. For large ξ, the action ressembles a "dipole" form [22, 3, 21]

$$S(\xi) = 1 - \frac{6}{\xi^2} + \mathcal{O}(\ln(\xi)/\xi^4). \qquad (27)$$

Finally, in this "dipole" approximation, the effective conformal parameter ξ_* and instanton size ρ_* entering Eqs. (24,25), read

$$\xi_* \simeq 2\,\frac{1+x}{1-x}, \qquad (28)$$

$$\rho_* \simeq \frac{4\pi}{\alpha_s(Q)Q}\frac{12}{\xi_*^2}. \qquad (29)$$

At this point a number of important remarks should be made.

Despite the complications associated with the γ^*-parton dynamics (c.f. Fig. 2), the gluon and quark structure functions (24,25) apparently exhibit the typical signatures of an individual I-subprocess cross section (18,19). Of course, the I-subprocess variables x', Q' appearing in Eqs. (18,19) are integrated over here (c.f. also Fig. 2) and effectively substituted by the appropriate γ^*-parton variables x, Q. Let us note, in particular, that the approximate expressions (28,29) agree with the solutions of the "saddle-point equations" – associated with the integrations over the collective coordinates – in case of an individual I-subprocess [3, 2].

The applicability of Eqs. (24,25) is restricted to sufficiently large x (c.f. Eq. (28)), since their derivation was based on the large ξ ("dipole") approximation (27) for the action. A further technical requirement is $1-x \gg \sqrt{\alpha_s(\rho_*^{-1})}$, excluding the neighbourhood of $x = 1$.

In general, the $I\overline{I}$ interaction, $U_{\rm int}(\xi_*) = S(\xi_*) - 1$, describes the emission and absorption of gluons from the instanton to the anti-instanton and vice versa (wavy lines between instanton and anti-instanton in Fig. 2). It generates via the Cutkovsky rules all final state tree-graph corrections to the leading semi-classical result (for a formal proof, see Ref. [23]). These final state corrections are well known to exponentiate [18]. However, it has been argued that some initial state and initial state – final state corrections exponentiate as well [24] and might give rise to additional corrections of order $4\pi/\alpha_s \mathcal{O}((1-x)^5)$ in the exponent.

The pre-exponential factor in Eqs. (24,25) is calculated only to leading accuracy in the strong coupling and up to corrections of order $\mathcal{O}(1-x)$. This is largely due to the fact, that $I - \overline{I}$ interactions have been essentially neglected in the prefactor, unlike the $I\overline{I}$ action in the exponent.

- On the one hand, this refers to the treatment of the "current quark" propagating in the $I\overline{I}$ background (c.f. Fig. 2). Its presence gives rise to great technical complications and, correspondingly, the results (24,25) only account for the first nontrivial terms in the cluster expansion [25] of the full current quark propagator in terms of the known propagator [26] in the background of a single (anti-)instanton.

- On the other hand, this refers to the evaluation of the functional determinants entering the pre-exponential factor. An improvement based on the $I\overline{I}$ valley is under way [27].

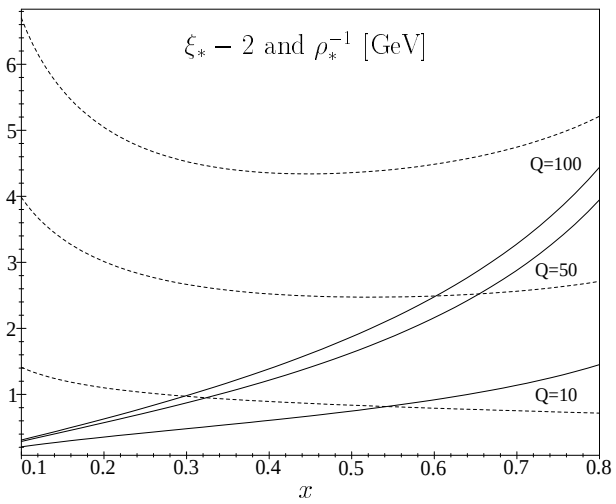

Figure 3: The effective conformal parameter $\xi_* - 2$ (solid) and inverse instanton size ρ_*^{-1} (dashed), obtained as solutions of the saddle point equations, Eq. (30), for a range of Q values (in GeV) and $n_f = 3$.

Despite these considerable formal restrictions in the derivation of the gluon and quark structure functions (24,25), it is tempting to try and evaluate these results within an experimentally accessible regime of $x_{\rm Bj}$ and Q^2. In order to hopefully enlarge the kinematical region where Eqs. (24,25) may be qualitatively trusted, we have heuristically applied the following "improvement" steps [4] (see also Ref. [1]):

- Throughout, in Eqs. (24,25), we use the $I\overline{I}$ valley action $S(\xi)$ of Refs. [3, 21], rather than its "dipole" approximation (27). This action represents an extension of Eq. (27) to arbitray values of $\xi \geq 2$. It is worth pointing out that it continuously interpolates between $S = 1$ (the sum of individual instanton and anti-instanton actions) at large ξ, and $S = 0$ for $\xi = 2$. These limiting situations correspond to a widely separated, non-interacting $I\overline{I}$-pair for $\xi \to \infty$ and the perturbative configuration of a collapsing and annihilating $I\overline{I}$-pair for $\xi \to 2$ (i.e. for $R \to 0, \rho_I = \rho_{\overline{I}}$).

- We replace the approximate expressions (28, 29) for the effective conformal parameter ξ_* and instanton size ρ_*, respectively, by the solu-

tions of the exact "saddle-point" equations [3, 2, 1],

$$\begin{aligned} \sqrt{\hat{s}}\rho_* &= \frac{8\pi}{\alpha_s(\rho_*^{-1})}\sqrt{\xi_*-2}\,S'(\xi_*)\,, \\ Q\rho_* &= \frac{4\pi}{\alpha_s(\rho_*^{-1})}(\xi_*-2)S'(\xi_*) - \rho_*\frac{\partial}{\partial\rho_*}\left(\frac{2\pi}{\alpha_s(\rho_*^{-1})}\right)S(\xi_*)\,, \end{aligned} \tag{30}$$

where $S'(\xi)$ is the derivative of the valley action $S(\xi)$ with respect to ξ. We have numerically solved Eqs. (30) (see Fig. 3), using the two-loop expression for the running coupling $\alpha_s(\rho_*^{-1})$ with three active flavors, and the value $\Lambda^{(3)}_{\overline{\rm MS}} = 365$ MeV. It corresponds to $\alpha_s(m_\tau) = 0.33$ [28].

The I-contribution to the nucleon structure function was finally obtained from convoluting the "improved" Eqs. (24,25) with very simple phenomenological expressions [29] for the gluon, u quark and d quark distributions, $g(z) = (3/z)(1-z)^5$, $u(z) = (2/\sqrt{z})(1-z)^3$, $d(z) = (1/\sqrt{z})(1-z)^3$, respectively. In view of the qualitative nature of this study, they turn out to be quite adequate for a factorization scale $\mu \simeq \rho_*^{-1}$, which is natural in this context. It turns out that over the whole $x_{\rm Bj}$ range considered the $\gamma^* g$ contribution to $F_2^{(I)}$ dominates. The sea-quark contributions can be neglected throughout the $x_{\rm Bj}$ range considered.

The resulting instanton-induced contribution to the structure function F_2 of the proton is displayed in Fig. 4. The expected very strong rise of the I-induced contribution with decreasing $x_{\rm Bj}$ is both apparent and suggestive!

Unfortunately, any further conclusions directly reflect the $(x_{\rm Bj}, Q^2)$ region where the above approximations are supposed to hold. For instance, the dashed lines in Fig. 4 define the boundaries of various "fiducial" regions corresponding to values of $S(\xi_*(x_{\rm Bj}, Q^2)) \geq 0.5, 0.4, 0.3$. As mentioned before, some authors [20] have advocated $F^{\rm QCD}_{\rm min} = S(\xi_*)_{\rm min} = 1/2$ as a saturating value for the holy grail function $F^{\rm QCD}$. The minimum value of Q considered in Fig. 4 is determined by the requirement that the effective instanton size should be sufficiently small. At $Q = 10$ GeV one finds $\rho_* \simeq 1$ GeV^{-1} (c.f. Fig. 3).

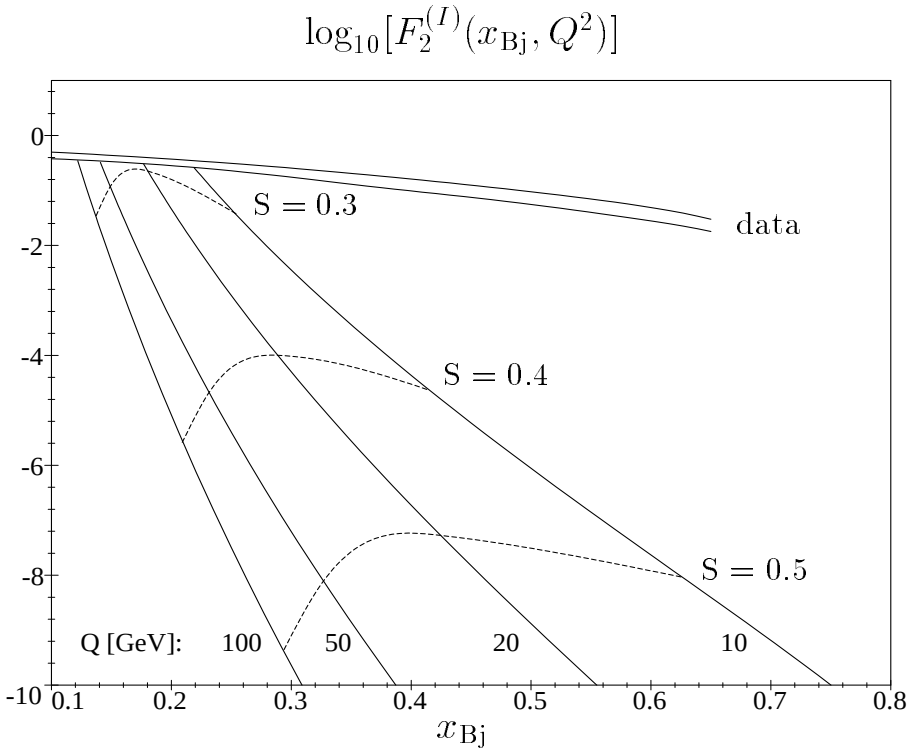

Figure 4: The logarithm of the instanton-induced contribution to the structure function F_2 of the proton, $\log_{10}[F_2^{(I)}(x_{\rm Bj}, Q^2)]$, Eq. (21), as a function of $x_{\rm Bj}$, for a range of Q values (in GeV) and $n_f = 3$. The curves denoted by "data" are to roughly represent the trend of the experimental data for F_2 within the same range of Q. The dashed curves correspond to constant values of the valley action, $S(\xi_*(x_{\rm Bj}, Q^2))$.

4 Phenomenology of Instanton Induced Particle Production at HERA

There are three main reasons which favour experimental searches for instanton-induced "footprints" in the multi-particle final state over searches via the structure functions, being the most inclusive observables in deep inelastic scattering.

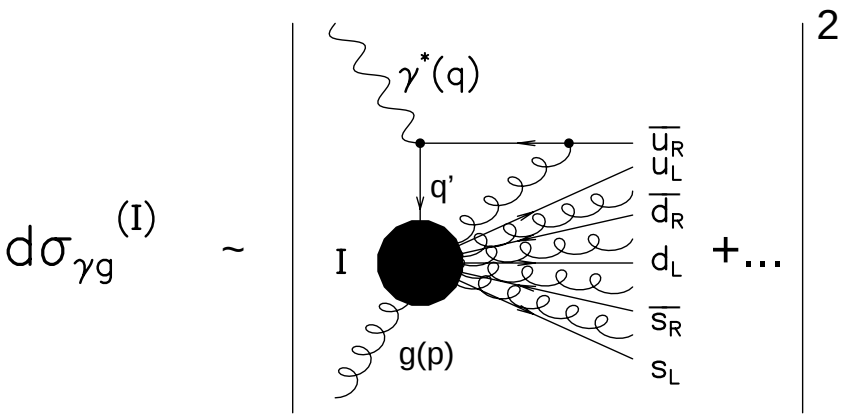

Figure 5: Graphical display of the instanton-induced contribution to the cross section of $\gamma^* g$ scattering for $\Delta Q^5 = 2n_f = 6$.

- On the one hand, the only experimental signal for QCD-instantons in the structure functions could be in form of an excess over the expected inclusive leptoproduction rate. However, enhancements at small $x_{\rm Bj}$ are also expected from other competing mechanisms like "(perturbative) Reggeization". Therefore, the structure functions are only of limited value in searches for manifestations of QCD-instantons.

- On the other hand, as we shall see, the instanton-induced *final state* is distinguished by a quite spectacular event topology together with a characteristic flow of flavour quantum numbers.

- Furthermore, the additional possibility of imposing experimental cuts on kinematical variables of the final state may well allow to restrict the I-subprocess variables $x', Q', \ldots$ within a theoretically controllable regime despite small $x_{\rm Bj}$. Along these lines one may hope to bridge the substantial gap between the regime of larger $x' \gtrsim \mathcal{O}(0.1)$, where the I-subprocess cross sections may be theoretically estimated, and the small $x_{\rm Bj}$ regime, $x_{\rm Bj} \lesssim O(10^{-3})$, where the bulk of HERA data is accumulating at present.

To elaborate on the last two aspects is the purpose of this Section.

A graphical display of the modulus squared of the relevant $\gamma^* g$ matrix element, along with various four-momenta of interest, is presented in Fig. 5. Its structure suggests that the instanton-induced contribution to the differential cross sections for $\gamma^* g(q) \to \cdots$ can be written in a "canonical" convolution form, as familiar from perturbative QCD:

$$d\sigma^{(I)}_{\gamma^* p}(x, Q^2, \ldots) \sim \sum_{p'} \int^{Q^2/x} \frac{dQ'^2}{Q'^2} \int_x^1 \frac{dx'}{x'} f^{(I)}_{\gamma^* p'} \left(\frac{x}{x'}, Q'^2 \right) d\sigma^{(I)}_{p' p}(x', Q'^2, \ldots). \tag{31}$$

The integrations in Eq. (31) extend over the variables x', Q'^2, referring as in Sect. 2 to the instanton-induced subprocess (denoted by I in Fig. 5),

$$\begin{aligned} Q'^2 &= -q'^2 \\ s' &= (q'+p)^2 \end{aligned} \qquad x' = \frac{Q'^2}{2pq'} = \frac{Q'^2}{s' + Q'^2}. \tag{32}$$

Their definition is completely analogous to the standard $e^{\pm} N$ variables $Q^2 = -q^2$ and $x_{\rm Bj} = Q^2/2Pq$ referring to the nucleon target of momentum P. The parton (gluon) momentum fraction with respect to the proton is $z = x_{\rm Bj}/x = (pq)/(Pq)$ and

$$0 < x_{\rm Bj} \leq x \leq x' \leq 1. \tag{33}$$

The conditions for the validity of Eq. (31) (beyond the set of approximations inherent in Ref. [1]), as well as a determination of the "splitting function" $f^{(I)}_{\gamma^* p'}(z', Q'^2)$, associated with the propagation of the current quark in the instanton background, are presently under active investigation [30]. To establish a structure of type (31) is quite an important task both from a theoretical point of view and also for further studies of instanton-induced phenomenology by means of Monte Carlo methods [31]. For the time being, we shall simply assume that Eq. (31) is valid approximately.

It is quite plausible that the "splitting function" $f^{(I)}_{\gamma^* p'}(z', Q'^2)$ in Eq. (31) only exhibits a relatively mild dependence on its variables. In contrast, the I-subprocess cross sections $d\sigma^{(I)}_{p' p}(x', Q'^2, \ldots)$ bring in the main dependences (of exponential type) and, of course, are most interesting from the physics point of view. Accordingly, we have concentrated our theoretical efforts in Ref. [4] on calculating the crucial observables characterizing the I-subprocess, such as normalized $1, 2, \ldots$-parton inclusive cross sections,

$$\frac{1}{\sigma^{(I)\,\rm tot}_{p' p}(x', Q'^2)} d\sigma^{(I)}_{p' p}(x', Q'^2, \ldots), \tag{34}$$

along with the respective average parton multiplicities, transverse momentum (flow), etc. Corresponding to the restrictions discussed in Sect. 3 in the context of the structure functions, the I-subprocess variables should not be too small, $x' \gtrsim \mathcal{O}(0.1)$, $Q' \gtrsim \mathcal{O}(10\ \mathrm{GeV})$, say.

Since a calculation of the "splitting function" in Eq. (31) is still under way [30], a discussion of expected event rates has to be deferred to a later stage. In the present analysis, we only make use of information abstracted from our calculations of the I-subprocess observables [4] along with HERA kinematics. This is sufficient, however, to obtain important insight into the expected event topology in the most interesting regime of small x_{Bj}. Moreover, the connection between kinematical quantities measurable in the laboratory system and the variables controlling the instanton subprocess may be studied.

Specifically, we use the following set of working hypotheses about the I-subprocess:
i) Isotropy: In its c.m. system, $\vec{q}'+\vec{p}=0$, the instanton-induced multi-parton production is supposed to proceed *isotropically*. We may imagine a "fireball" in S-wave configuration, decaying into gluons and at least $2n_f-1$ quarks, including *strangeness* (!) and possibly charm, if kinematically allowed (c.f. Fig. 5).
ii) Dependence on x', Q'^2: The I-subprocess cross sections $d\sigma^{(I)}_{p'_p}(x', Q'^2, \ldots)$ are expected to strongly decrease with increasing Q'^2 for fixed x' and to strongly increase with decreasing x' for fixed Q'^2 (c.f. Sect. 2). As discussed above and in Sect. 3, it remains uncertain, however, how long the cross sections continue to increase towards $x' \to 0$.
iii) Multiplicity: The total multiplicity associated with the I-subprocess is expected to be large,

$$\langle n_{\mathrm{g+q}}(x', Q'^2)\rangle \sim \mathcal{O}\left(\frac{\pi}{2\alpha_s}\right) + 2n_f - 1 \gtrsim \mathcal{O}(10), \tag{35}$$

on the parton level, leading typically to $\mathcal{O}(20 \div 30)$ particles after hadronization. In Fig. 6, we display $\langle n_{\mathrm{g+q}}(x', Q'^2)\rangle$ as calculated in Ref. [4].

At small values of x' and large Q'^2, the multiplicity obtains a large contribution from gluons and peaks around $x' \approx 0.2 \div 0.3$, whereas at large x' the $2n_f - 1 = 5$ produced quarks dominate. The peaking of the gluon multiplicity at small, non-vanishing x' actually has an appealing interpretation:

For large values of Q'^2 the coefficient of $\pi/2\alpha_s$ in Eq. (35) turns out to be [4] $4(\xi_* - 2)\, S'(\xi_*)$, involving the derivative of the valley ac-

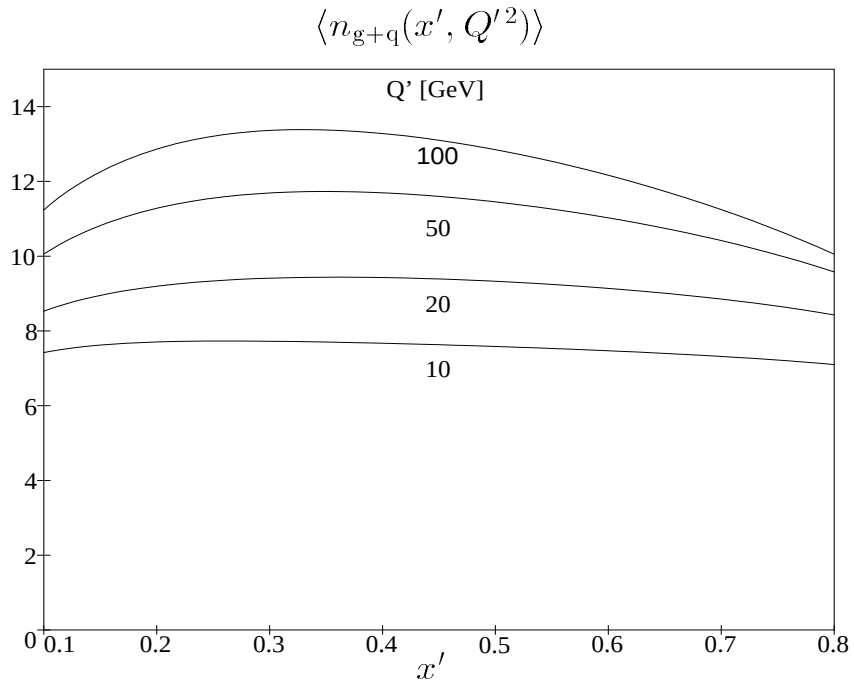

Figure 6: The average, total parton multiplicity associated with the I-subprocess as a function of x', for different values of Q' and $n_f = 3$, from Ref. [4].

tion with respect to the conformal parameter ξ, taken at the saddle point value $\xi_*(x', Q'^2)$ (c.f. Fig. 3). As discussed in Sect. 3, the full valley action smoothly interpolates between a non-interacting, infinitely separated instanton/anti-instanton pair for $\xi \to \infty$ (probed for $x' \to 1$) and the perturbative vacuum for $\xi \to 2$ (probed for $x' \to 0$). Hence, in both limits a *decrease* of the gluon multiplicity matches well the intuition! The peak of the multiplicity inbetween corresponds to the maximal variation of the action with ξ.

We also note the substantial increase of the gluon multiplicity with increasing Q'^2, which at large Q'^2 mainly reflects the running of α_s in Eq. (35).

iv) $k_\perp$ signature: The transverse momenta of the partons emerging from the instanton subprocess and the one of the current-quark jet (c.f. Fig. 5) are

expected to be "semi hard", typically of order [4, 1]

$$|k_{\perp i}| \sim \frac{< k_{\perp \,\mathrm{tot}} >}{< n >} = \frac{\pi}{4}\frac{\sqrt{s'}}{< n >} \sim \alpha_s \frac{\sqrt{s'}}{2};\ i \subset I, \ \text{and} \tag{36}$$

$$|k_{\perp \,\text{current quark}}| \sim \sqrt{\alpha_s Q^2}. \tag{37}$$

Given this plausible generic input *i) - iv)*, we may now ask, how instanton-induced events would look like in the H1/ZEUS detectors.

First of all, we observe that as a direct consequence of the *isotropy* assumption *i)*, the (pseudo) rapidity distribution of a single final state parton in the I-c.m. system takes the form

$$\frac{1}{\sigma^{(I)\,\mathrm{tot}}}\frac{\mathrm{d}\sigma^{(I)}(x', Q'^2, \eta_I)}{\mathrm{d}\eta_I \mathrm{d}\phi_I} = \frac{1}{4\pi}\frac{< n(x', Q'^2) >}{\cosh(\eta_I)^2}, \tag{38}$$

i.e. it is strongly peaked in (pseudo) rapidity $\eta_I = -\ln\tan(\theta_I/2)$ around $\eta_I = 0$ with a half width of

$$\Delta\eta_I \approx \pm 0.9. \tag{39}$$

The shape and width of the distribution in pseudo rapidity remains, of course, very similar in the HERA laboratory system, for kinematical configurations where the I-c.m. system is dominantly boosted longitudinally. Depending on the values of the various subprocess variables, the peak position ($\eta_I = 0$) fluctuates in general over the available range of η^{lab} (for given x_{Bj} and y viz. Q^2):

$$\begin{aligned}\eta_I^{\mathrm{lab}} &= \frac{1}{2}\ln\left(\frac{E_P}{yE_e}\frac{x_{\mathrm{Bj}}}{x_\gamma}\left[\frac{1-x'}{x} + x_\gamma(1-y) + (1-x_\gamma)(\frac{x'}{x}-1)\right.\right. \\ &\left.\left. -2\sqrt{(1-y)x_\gamma(1-x_\gamma)(\frac{x'}{x}-1)}\cos\,\chi\right]\right).\end{aligned} \tag{40}$$

In analogy to the standard y variable, we have introduced in Eq. (40) the q' momentum fraction

$$0 < x_\gamma = \frac{q'p}{qp} < 1. \tag{41}$$

The variable χ denotes the azimuthal angle of the vector $\vec{q'}$ in the HERA laboratory frame. Due to momentum conservation, $|\vec{q}'_\perp|\sin\chi = -k_{y\,\text{current quark}}$,

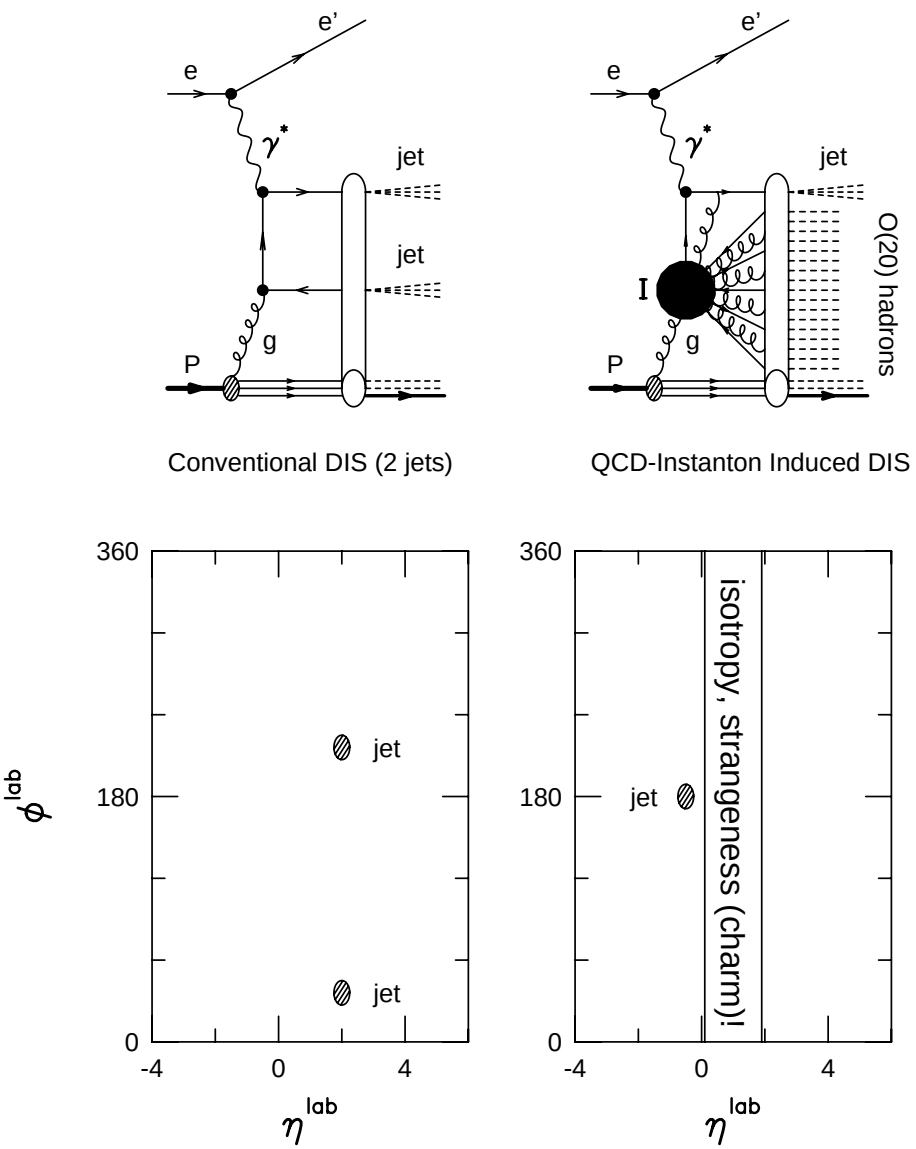

Figure 7: The dominant matrix element and $(\eta^{\rm lab}, \phi^{\rm lab})$-plot of a typical instanton-induced event is contrasted with the canonical two-jet configuration in perturbative QCD.

the component of the current-quark momentum out of the $ee'P$ scattering plane.

In Fig. 7, the dominant matrix element and $(\eta^{\rm lab}, \phi^{\rm lab})$-plot of a typical instanton-induced event is contrasted with the canonical two-jet configuration in perturbative QCD.

Clearly, the "0th level" signature to watch out for is a densely populated hadronic "band" in the $(\eta^{\rm lab}, \phi^{\rm lab})$-plane, centered at a fluctuating value (40) of $\eta_I^{\rm lab}$. This striking multi-hadron final state originates from $8 \div 10$ "semi-hard" jets (c.f. Fig. 6), always includes strangeness and is characterized by a width $\triangle\eta_I^{\rm lab} = \pm 0.9$. Let us point out two observables, which – on an event-by-event basis – appear to be particularly sensitive to this event structure.

- *The (transverse) energy flow*, $\mathrm{d}E_{(\perp)}/\mathrm{d}\eta^{\rm lab}$ (integrated over $\phi^{\rm lab}$), will exhibit a strong enhancement at the position $\eta^{\rm lab} = \eta_I^{\rm lab}$ of the "band", since each of the $8 \div 10$ instanton-induced jets contributes a comparable energy into a single $\eta^{\rm lab}$ bin of width ≈ 1.8. If, in addition, the current-quark jet is isolated from the "band" (see below), one even expects a double-peak structure in $\mathrm{d}E_{(\perp)}/\mathrm{d}\eta^{\rm lab}$. The energy flow signature may well be less affected by hadronization than patterns associated with individual tracks.

- *Pseudo sphericity*: The usual event-shape variables like sphericity and aplanarity should be useful tools in analysing the manifestations of an isotropic instanton-induced subprocess in the final state. Of particular sensitivity appears the so-called pseudo sphericity [32], which incorporates only transverse information from the event in terms of the azimuthal angles ϕ_i of the N final state hadrons:

$$\text{Pseudo sphericity} = 1 - \frac{1}{N}\sqrt{(\sum_{i=1}^{N}\cos\phi_i)^2 + (\sum_{i=1}^{N}\sin\phi_i)^2}. \qquad (42)$$

  Apparently, it equals to 1 in the c.m. system of an isotropical event and vanishes for a single "collimated" jet.

As a next level of sophistication, we study the effects of kinematical cuts on suitable final-state variables with the aim, to further enhance the event topology and to unfold and/or restrict the I-subprocess variables x', Q'. Of course, this has to be achieved

- without affecting significantly the expected size of the I-subprocess cross section $\mathrm{d}\sigma^{(I)}$ (by exploring input *ii)* above);

- such that the I-subprocess is invoked in a kinematical region of (x', Q'), where it induces a high average multiplicity $\langle n_{\mathrm{g+q}} \rangle$ according to Fig. 6.

The key aspect is to focus on an event topology corresponding to an *isolated* (semi-hard) current-quark jet (c.f. input *iv)* above: $k_\perp \approx \sqrt{\alpha_s Q^2}$) *in addition to* a hadronic "band" in $(\eta^{\mathrm{lab}}, \phi^{\mathrm{lab}})$ as discussed in "level 0" above. To this end, let us consider the constraints on the (internal) subprocess variables x_γ, x', $Q' \ldots$, implied by the following reasonable separation criteria:

- The hadronic "band" should be contained in the (central) detector, such that its peak position satisfies $|\eta_I^{\mathrm{lab}}| \lesssim 1$, say (in practice, this upper bound for η_I^{lab} may well be pushed up to ~ 2).

- The current-quark jet is required to be separated in η^{lab} from the hadronic "band" (centered around η_I^{lab}) by

$$\triangle\eta \equiv \eta_I^{\mathrm{lab}} - \eta_{\mathrm{current\ quark}}^{\mathrm{lab}} \begin{cases} \lesssim -1.5 \text{ or} \\ \gtrsim +1.5 \end{cases} \tag{43}$$

- A minimal transverse momentum, $k_{\perp\,\mathrm{current\ quark}} \gtrsim 4$ GeV, is required for the current-quark jet.

In Fig. 8 we have displayed the resulting restrictions on the internal subprocess variables x_γ, x', for a typical set of fixed "external" parameters x_{Bj},y,x. Apparently, after imposing the isolation requirements for the current-quark jet we are left with two allowed, 'triangular' regions 1 and 2, in the (x_γ, x')-plane. The central portion of Fig. 8 is excluded by the cut on $\triangle\eta$ (solid lines), with the left- (right-) hand boundary corresponding to $\triangle\eta = +1.5$ (-1.5). The excluded portion on the left (short dashes) refers to the hadronic "band" being centered within $1 \leq \eta_I^{\mathrm{lab}} \leq 2.2$, with $\eta_I^{\mathrm{lab}} = 1$ located on the right. Hence, if a value of η_I^{lab} *above* 1 is experimentally tolerable, the allowed region 1 increases significantly. Finally, the main effect of the requirement $k_{\perp\ \mathrm{current\ quark}} \geq 4$ GeV , is to set a lower limit to the involved values of x', and to exclude the region x_γ very close to 1 (long dashes).

These results demonstrate that, indeed, kinematical cuts of the type considered here, may well restrict the I-subprocess variables x', Q' to regions

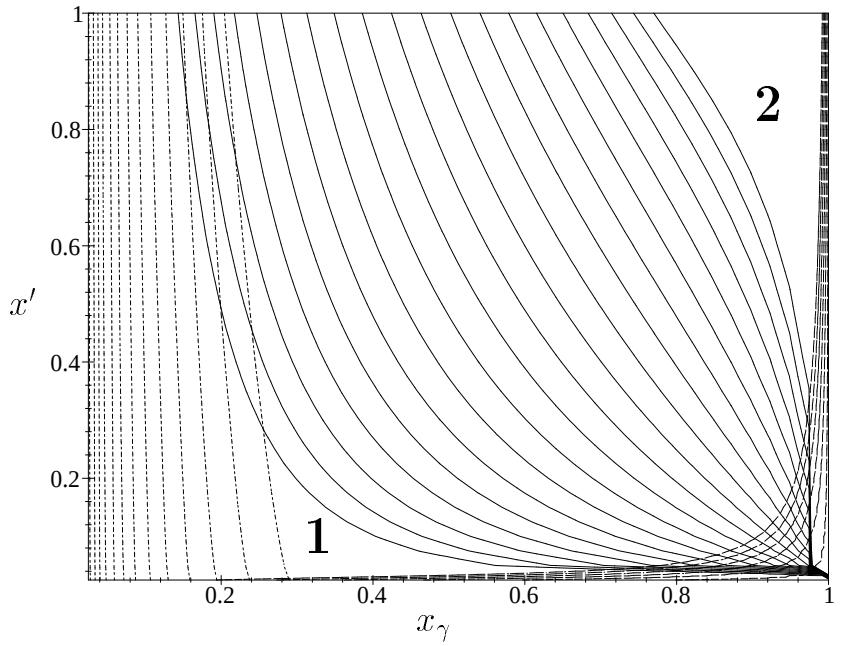

Figure 8: In the displayed regions $1, 2$ of the (x_γ, x')-plane, the current-quark jet is isolated from the instanton-induced "band" (centered at $\eta_I^{\rm lab}$). The excluded domains are: $-1.5 \leq \triangle\eta \equiv \eta_I^{\rm lab} - \eta^{\rm lab}_{\text{current quark}} \leq 1.5$ (solid lines), $1 \leq \eta_I^{\rm lab}$ (short dashes) and $k_{\perp \text{ current quark}} \leq 4$ GeV (long dashes). The parameters are $E_p = 820$ GeV, $E_e = 30$ GeV, $x_{\rm Bj} = 0.001$, $y = 0.5$ ($Q = 7$ GeV), $x = 0.025$ ($\sqrt{\hat{s}} = 44$ GeV) and $\vec{q}'$ azimuthal angle $\chi = 0$.

where the computation [4] of $d\sigma^{(I)}_{p'p}(x', Q')$ may be trusted (e.g. within regime 2 of Fig. 8).

According to our input *ii)* above and Fig. 9, regime 1 in Fig. 8 will presumably be associated with considerably higher rates, since it typically corresponds to much smaller values of Q' and x' than regime 2. From Fig. 9 we also infer a comfortably high total parton multiplicity $\langle n_{\rm g+q}\rangle \approx 8$ in regime 1, as well as an energy/parton $= \sqrt{s'}/8 \gtrsim 3$ GeV in the I-c.m. system.

Let us finally illustrate in Figs. 10, 11 an event in the HERA laboratory frame, corresponding both to a striking signature (isolated current-quark jet along with a densely populated hadronic "band") and favourable rate/multiplicity conditions for the instanton subprocess. We note the corre-

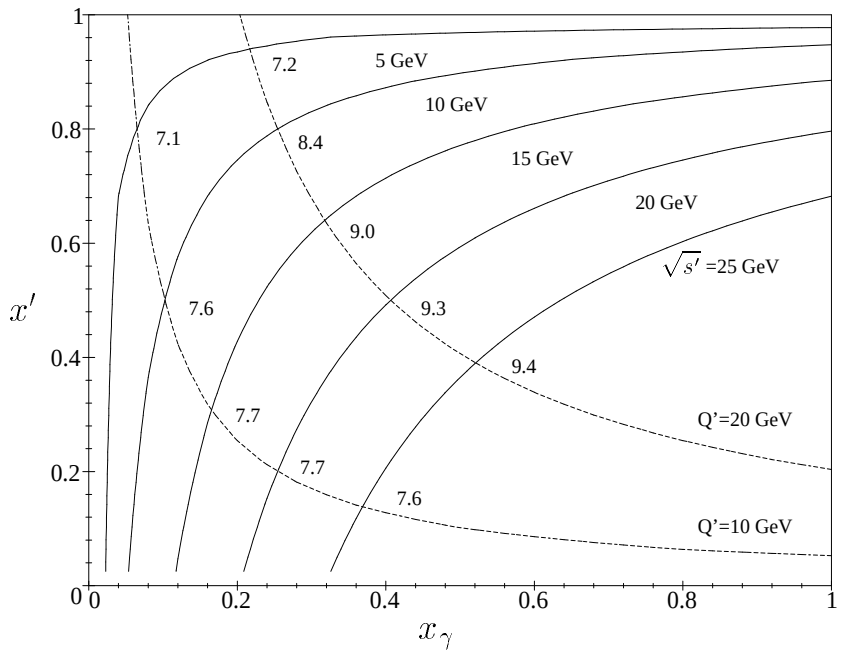

Figure 9: Lines of constant invariant mass of the I-subprocess, $\sqrt{s'}$, and constant Q' (dashed), versus the subprocess variables x' and x_γ, for the same parameters as in Fig. 8. The numbers at the crossing points denote the respective I-subprocess multiplicities $\langle n_{\mathrm{g+q}} \rangle$ according to Fig. 6.

sponding event-shape variables (on the parton level in the laboratory frame) as calculated from the instanton-induced partons within the "band"

$$\begin{aligned} \mathrm{Sphericity}^{(I)}_{|\mathrm{lab}} &\approx 0.45, \\ \mathrm{Aplanarity}^{(I)}_{|\mathrm{lab}} &\approx 0.22, \\ \mathrm{Pseudo\ sphericity}^{(I)}_{|\mathrm{lab}} &\approx 0.90. \end{aligned} \tag{44}$$

Of course, due to the isotropy of the instanton-induced subprocess, the sphericity, aplanarity and pseudo-sphericity variables essentially adopt their maximal values of 1, 1/2 and 1, respectively, in the I-c.m. frame. Apparently, the pseudo sphericity is least affected by the Lorentz transformation into the laboratory frame and continues to reflect the underlying isotropy. Clearly, for a quantitative discussion, hadronization effects have

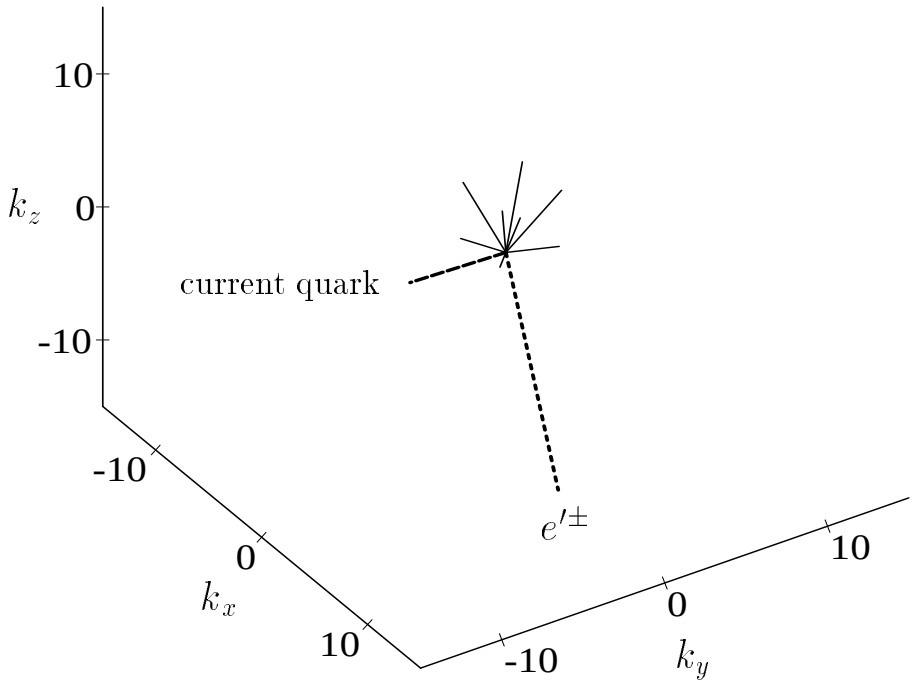

Figure 10: 3d-momentum display (in GeV) for a typical instanton-induced event before hadronization, in the HERA laboratory frame, satisfying the kinematical cuts discussed in the text. The current-quark jet is well isolated. Not shown are the incoming proton ($+z$ direction) and $e^{\pm}$ ($-z$ direction), as well as the proton fragments. The parameters are as in Fig. 8 and moreover, $x_\gamma = 0.32$, $x' = 0.1$, such that $Q' \approx 8$ GeV, $\sqrt{s'} \approx 24$ GeV and $\langle n_{\mathrm{g+q}} \rangle \approx 8$.

to be included[31], which may well wash out somewhat the traces of the underlying isotropy in the various event shape parameters.

5 Summary and Outlook

The search for QCD-instanton induced events at HERA is well worth the effort:

First of all, these "anomalous" processes are predicted to occur *within standard QCD*. Secondly, there is a close analogy to electroweak $B+L$

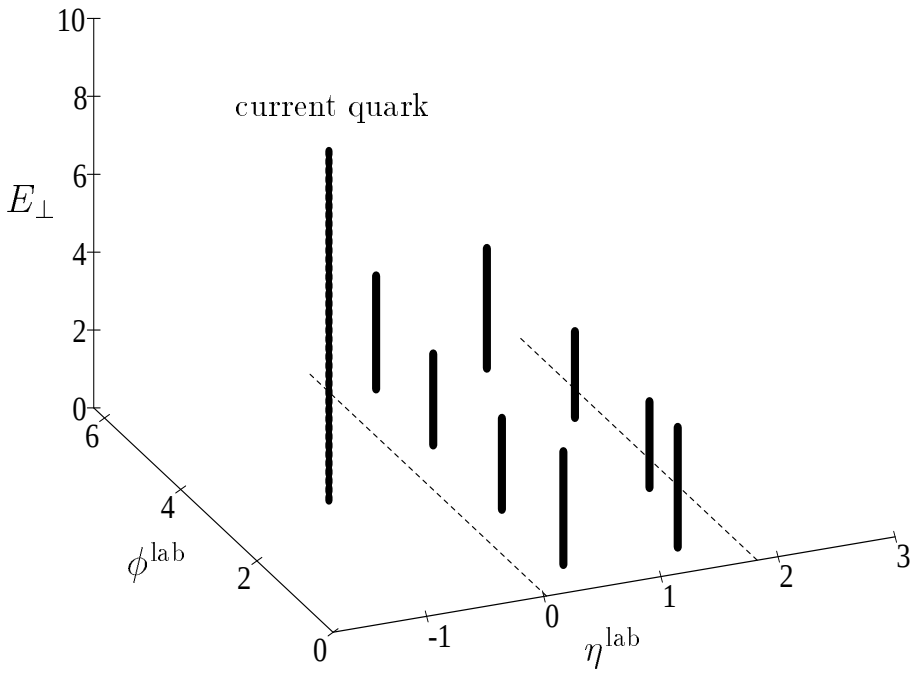

Figure 11: Lego plot of the transverse energy in GeV (before hadronization) for the same instanton-induced event as in Fig. 10, satisfying the kinematical cuts discussed in the text. Not shown are the scattered $e^\pm$ and the proton fragments.

violating processes, as was discussed in detail in Sect. 2. While a promising search for anomalous electroweak events is only possible in the far future, the search for manifestations of QCD-instantons can start right now, in deep inelastic $e^\pm p$ scattering at HERA.

Besides summarizing the essence and limitations of the theoretical calculations involved [1], we have presented in Sect. 3 a state of the art evaluation of the instanton-induced contribution to the nucleon structure function F_2. It rises strongly with decreasing $x_{\rm Bj}$ and tends to reach the size of the experimental data around $x_{\rm Bj} \approx 0.1 \div 0.25$. Unfortunately, due to inherent uncertainties, the calculation cannot be trusted anymore for $x_{\rm Bj} \lesssim 0.35$, say. Nevertheless, the trend is very suggestive! However, enhancements of the inclusive leptoproduction rate at small $x_{\rm Bj}$ are also expected from other competing mechanisms like "(perturbative) Reggeization". Therefore, the

structure functions appear only of limited value in searches for "footprints" of QCD-instantons.

In Section 4 we have reported first phenomenological results of our ongoing broad and systematic investigation of the QCD-instanton induced *hadronic final state* [4]. Since a calculation of the "splitting function" – associated with the propagation of the current quark in the instanton background – is still in progress, a discussion of expected event rates has to be deferred to a later stage. In the present analysis we only made use of information abstracted from our calculation of the instanton-subprocess observables [4] along with HERA kinematics. This was sufficient, however, to obtain important insight into the expected event topology in the most interesting regime of small $x_{\rm Bj}$.

- The "0th level" signature to watch out for is a densely populated hadronic "band" in the $(\eta^{\rm lab}, \phi^{\rm lab})$-plane (c.f. Fig. 7), centered at some fluctuating value $\eta_I^{\rm lab}$. This striking multi-hadron final state originates from $8 \div 10$ "semi-hard" jets (c.f. Fig. 6), always includes strangeness and is characterized by a width $\triangle\eta_I^{\rm lab} = \pm 0.9$. It directly reflects an underlying instanton-subprocess, associated with the formation of an S-wave "fireball", which then decays isotropically into gluons and at least $2n_f - 1$ quarks. Observables which are particularly sensitive to this event structure are e.g. the (transverse) energy flow and the so-called pseudo sphericity. The energy flow signature may well be less affected by hadronization than patterns associated with individual tracks.

- As a next level of sophistication, we have studied kinematical cuts on suitable final-state variables, which help to further enhance the event topolology and to unfold and/or restrict the (Bjorken) variables of the instanton subprocess within a theoretically controllable regime, despite small $x_{\rm Bj}$. Along these lines one may hope to bridge the substantial gap between the kinematical region, where the instanton-subprocess cross sections may be theoretically estimated [4], and small $x_{\rm Bj}$ values, $x_{\rm Bj} \lesssim O(10^{-3})$, where the bulk of HERA data is accumulating at present.

In summary, experimental searches for instanton "footprints" in the multiparticle final state appear to be much more promising than searches via the structure functions.

Finally, let us briefly mention some related theoretical and phenomenological issues presently under study. Theoretical work is in progress to improve the pre-exponential factors, affecting quite strongly the predictions for structure functions and the various subprocess cross sections. This refers in particular to a more reliable evaluation of the functional determinants [27] in the instanton/anti-instanton valley background beyond the dilute instanton-gas approximation.

Of great importance for further studies of QCD-instanton phenomenology is the task of establishing a convolution form [30] of the γ^*-parton multi-particle cross sections in terms of "splitting functions" and instanton-subprocess cross sections (c.f. Eq. (31)). Once the "splitting functions" have been isolated and calculated, we hope to come forward with predictions for the rate of instanton-induced multi-particle events. We are then ready to study the instanton-induced multi-particle final state by means of a Monte Carlo based event generator [31]. Only after including effects of hadronization and background will it be possible to address the crucial question: How many "anomalous" events are needed to establish the "discovery" of an instanton at HERA?

Acknowledgements

We would like to thank W. Bartel, T. Haas, M. Kuhlen and A. de Roeck for many useful suggestions on experimental issues. Furthermore, we would like to acknowledge helpful discussions with V. Braun, S. Moch, G. Schuler and C. Wetterich.

References

[1] I. Balitsky and V. Braun, *Phys. Lett.* **B314** (1993) 237.

[2] I. Balitsky and V. Braun, *Phys. Rev.* **D47** (1993) 1879.

[3] V.V. Khoze and A. Ringwald, *Phys. Lett.* **B259** (1991) 106.

[4] A. Ringwald and F. Schrempp, *in preparation.*

[5] G. 't Hooft, *Phys. Rev. Lett.* **37** (1976) 8; *Phys. Rev.* **D14** (1976) 3432.

[6] A. Ringwald, *Nucl. Phys.* **B330** (1990) 1;
O. Espinosa, *Nucl. Phys.* **B343** (1990) 310.

[7] For a review, see:
M. Mattis, *Phys. Rep.* **214** (1992) 159;
P. Tinyakov, *Int. J. Mod. Phys.* **A8** (1993) 1823;
R. Guida, K. Konishi, N. Magnoli, *Int. J. Mod. Phys.* **A9** (1994) 795;
I. Balitsky, talk presented at the Workshop 'Continuous Advances in QCD', Minneapolis, 18-20 February 1994, Penn State University preprint PSU/TH/146 (May 1994), hep-ph 9405335.

[8] G. Farrar and R. Meng, *Phys. Rev. Lett.* **65** (1990) 3377;
A. Ringwald, F. Schrempp and C. Wetterich, *Nucl. Phys.* **B365** (1991) 3;
M. Gibbs, A. Ringwald, B. Webber and J. Zadrozny, CERN preprint CERN-TH.7090/93 (June 1994), hep-ph 9406266.

[9] D. Morris and R. Rosenfeld, *Phys. Rev.* **D44** (1991) 3530;
D. Morris and A. Ringwald, *Astropart. Phys.* **2** (1994) 43.

[10] R. Jackiw and C. Rebbi, *Phys. Rev. Lett.* **37** (1976) 172;
C. Callan, R. Dashen and D. Gross, *Phys. Lett.* **B63** (1976) 334.

[11] N. Manton, *Phys. Rev.* **D28** (1983) 2019; F. Klinkhamer and N. Manton, *Phys. Rev.* **D30** (1984) 2212.

[12] H. Aoyama and H. Goldberg, *Phys. Lett.* **B188** (1987) 506;
P. Arnold and L. McLerran, *Phys. Rev.* **D37** (1988) 1020.

[13] I. Balitsky and V. Braun, DESY preprint DESY 94-179 (October 1994), hep-ph 9410271.

[14] S. Adler, *Phys. Rev.* **177** (1969) 2426;
J. Bell and R. Jackiw, *Nuovo Cimento* **51** (1969) 47;
W.A. Bardeen, *Phys. Rev.* **184** (1969) 1848.

[15] A. Belavin, A. Polyakov, A. Schwarz and Yu. Tyupkin, *Phys. Lett.* **B59** (1975) 85.

[16] I. Affleck, *Nucl. Phys.* **B191** (1981) 429.

[17] N. Andrei and D. Gross, *Phys. Rev.* **D18** (1978) 468;
L. Baulieu, J. Ellis, M. Gaillard and W. Zakrzewski, *Phys. Lett.* **B77**

(1978) 290; *ibid.* **B81** (1979) 41;
T. Appelquist and R. Shankar, *Phys. Rev.* **D18** (1978) 2952;
V. Novikov, M. Shifman, A. Vainshtein and V. Zakharov, *Nucl. Phys.* **B174** (1980) 378;
M. Dubovikov and A. Smilga, *Nucl. Phys.* **B185** (1981) 109.

[18] L. Yaffe, in: Proc. of the Santa Fe Workshop on Baryon Number Violation at the SSC?, eds. M. Mattis and E. Mottola, (World Scientific, Singapore, 1990), pp. 46-63.
P. Arnold and M. Mattis, *Phys. Rev.* **D42** (1990) 1738;
S. Khlebnikov, V. Rubakov and P. Tinyakov, *Nucl. Phys.* **B350** (1991) 441.

[19] V. Zakharov, Minnesota preprint TPI-MINN-07/7-T (1990) (unpublished); *Nucl. Phys.* **B371** (1992) 637;
M. Porrati, *Nucl. Phys.* **B347** (1990) 371;
S. Khlebnikov, V. Rubakov and P. Tinyakov, *Nucl. Phys.* **B350** (1991) 441;
V.V. Khoze and A. Ringwald, *Nucl. Phys.* **B355** (1991) 351;
P.Arnold and M.Mattis, *Phys. Rev.* **D44** (1991) 3650;
A. Mueller, *Nucl. Phys.* **B364** (1991) 109;
D. Diakonov and V. Petrov, in: Proc. of the XXVIth LNPI Winter School, (Leningrad, 1991), pp. 8-64;
I. Balitsky and A. Schäfer, *Nucl. Phys.* **B404** (1993) 639;
P. Silvestrov, *Phys. Lett.* **B323** (1994) 25.

[20] V. Zakharov, *Nucl. Phys.* **B353** (1991) 683;
M. Maggiore and M. Shifman, *Nucl. Phys.* **B365** (1991) 161;
G. Veneziano, *Mod. Phys. Lett.* **A7** (1992) 1661;
D. Diakonov and V. Petrov, *Phys. Rev.* **D50** (1994) 266.

[21] A. Yung, *Nucl. Phys.* **B297** (1988) 47;
V.V. Khoze and A. Ringwald, *Phys. Lett.* **B259** (1991) 106;
V.V. Khoze and A. Ringwald, CERN preprint CERN-TH.6082/91 (unpublished);
J. Verbaarschot, *Nucl. Phys.* **B362** (1991) 33;
I. Balitsky and V. Braun, *Nucl. Phys.* **B380** (1992) 51.

[22] C. Callan, R. Dashen and D. Gross, *Phys. Rev.* **D17** (1978) 2717.

[23] P. Arnold and M. Mattis, *Phys. Rev.* bf D44 (1991) 3650.

[24] A. Mueller, *Nucl. Phys.* **B348** (1991) 310; *Nucl. Phys.* **B353** (1991) 44.

[25] E. Mottola, *Phys. Rev.* **D17** (1978) 1103;
N. Andrei and D. Gross, *Phys. Rev.* **D18** (1978) 468.

[26] L. Brown, R. Carlitz, D. Creamer and C. Lee, *Phys. Rev.* **D17** (1978) 1583.

[27] J. Fuchs, A. Ringwald and F. Schrempp, *work in progress.*

[28] D. Buskulic et al. (ALEPH Collaboration), *Phys. Lett.* **B307** (1993) 209.

[29] G. Schuler, *private communication.*

[30] S. Moch, A. Ringwald and F. Schrempp, *work in progress.*

[31] M. Gibbs, A. Ringwald and F. Schrempp, *work in progress.*

[32] P. Carlson, in: Proc. 4th Workshop on $\bar{p}p$ collider physics (Bern 1984), CERN Yellow Report 84-09, p. 286;
J. Rushbrooke, in: Workshop on $\bar{p}p$ options for the supercollider (SSC), (University of Chicago, February 1984), p. 176;
Ch. Geich-Gimbel, in: The quark structure of matter, (Strassburg-Karlsruhe, 1985), (World Scientific, 1986), p. 465.